Optical Materials 31 (2009) 701–706

Contents lists available at ScienceDirect

Optical Materials

journal homepage: www.elsevier.com/locate/optmat

Ceramic laser materials and the prospect for high power lasers

V. Lupei *

Institute of Atomic Physics-INFLPR, Laboratory of Solid-State Quantum Electronics, Bucharest 077125, Romania

ARTICLE INFO

Article history:
Available online 5 June 2008

Keywords:
Laser materials
Transparent ceramics
Solid-state lasers

ABSTRACT

The paper discusses the possibilities for enhancement of laser emission parameters and power scaling of Nd-doped transparent ceramic materials. It is shown that by a correlated approach that accounts for the properties of the laser material, pumping conditions and details of laser design, the direct diode laser pumping of these lasers into the emitting level $^4F_{3/2}$ enables additional power scaling in the range of 50–60% compared with the traditional 800 nm pumping in $^4F_{5/2}$.

1. Introduction

The extended capabilities of the ceramic laser materials compared with the single crystals (larger size, increased compositional versatility, higher doping concentrations with controlled profile and so on) offer potential for extension of the performances of solid-state lasers. The Nd:YAG ceramic laser rods show currently comparable or even better emission characteristics than the similar (size, doping concentration) single crystal rods [1–3]. Moreover, they enable considerable extension of performances: the use of large ($10 \times 10 \times 2$ cm^3) 0.3 at.% Nd:YAG ceramic components under quasi-CW 809 nm diode laser pumping enhanced the power capabilities of the heat capacity lasers in burst regime [4] from 27 kW, obtained with Nd:GGG crystals, to 67 kW. Further scaling to higher power of this laser in the actual configuration is prevented by the heating effects.

This paper analyses some of the directions for improvement of performances of the lasers based on transparent ceramics of Nd-doped garnets, with particular accent on Nd:YAG and Nd:GSGG as materials for high power CW and, respectively, high-energy Q-switched pulse laser emission. The transparent ceramic materials enable good control of pump absorption and utilization of pumping schemes that enhance the laser performances and reduce drastically the generation of heat by non-radiative processes. In principle, the direct pumping into the emitting level $^4F_{3/2}$ of the Nd-doped laser materials could improve the laser parameters expressed in absorbed pump power by ~10% simultaneously with the reduction of heat generation by ~30% in case of the one-micron $^4F_{3/2} \rightarrow {}^4I_{11/2}$ laser emission and by ~50% for the efficient quasi-three-level $^4F_{3/2} \rightarrow {}^4I_{9/2}$ lasers [5–7]. A proper account of the effect of this approach on the laser performances expressed vs. the incident pump power must account for the possible effects on other properties of the laser material, especially on the absorption efficiency. Thus conditions that overcome the reduced pump absorption into the emitting level $^4F_{3/2}$ of Nd^{3+} in garnets must be granted and this can be accomplished by using YAG ceramics with enhanced Nd concentrations C_{Nd} or/and large size or by recirculation of the pump radiation inside the laser material [8]. However, increased C_{Nd} could reduce the emission quantum efficiency due to the energy transfer between the Nd ions, with deleterious effect on the laser emission threshold and on the global optical-optical efficiency as well as on the heat generation.

The selection of the material parameters (C_{Nd}, size) and of pump conditions (wavelength, intensity) that would grant optimal balance between the useful and the deleterious effects on the laser performances can be facilitated by definition of several figures of merit of gradually increased complexity. These figures of merit require the accurate knowledge of the C_{Nd} dependence of the emission quantum efficiency and this can be calculated with the energy transfer parameters inferred from the emission decay. For the investigated garnet materials the energy transfer parameters for the ceramics are similar to those for the single crystals and the effect is larger in case of Nd:YAG [9] than for Nd:GSGG [10].

The selection of the material and of the pumping characteristics by using such figures of merit is illustrated for the continuous-wave Nd:YAG lasers, but the conclusion of the analysis can be extended to other types of Nd lasers. This analysis indicates that a correlated selection of the material parameters and of the pumping condition could grant the power scaling of these lasers by more than 50% compared with the traditional 809 nm pumping.

2. Ceramic laser materials

The polycrystalline transparent materials produced by ceramic techniques are fully dense bodies composed of tightly packed, ran-

* Tel./fax: +40 21 457 4472.
E-mail addresses: v.lupei@pluto.infim.ro, lupei_voicu@yahoo.com.

0925-3467/$ - see front matter © 2008 Elsevier B.V. All rights reserved.
doi:10.1016/j.optmat.2008.04.007

domly oriented crystalline grains of uniform size, with shallow grain boundaries and with very low volume densities of nanometer-size inter-grain pores. The size of the ceramic grains is important since it could influence the optical, mechanical and thermal properties of the ceramic material. It also determines the ratio between the surface and the volume of the grains and thus it controls the extent of the possible deleterious effects of the surface. The transparent ceramic approach could be particularly useful in case of the refractory cubic oxide materials such as garnets and sesquioxides, whose high melting point (around 1900–2000 °C and 2400 °C, respectively) limits severely the possibilities to grow large crystals of high optical quality by methods based on the crystallization from melt. In case of garnets, the early attempts to produce transparent ceramics by conventional sintering resulted in translucent materials with large density of inter-grain pores that prevented laser emission. It was only in 1995 when Ikesue et al. [1] demonstrated that the density of pores could be drastically reduced by isostatic compression before the final vacuum sintering stage at 1700 °C. Similar approach was used to produce highly transparent Y_2O_3 ceramics [11]. In this technique the synthesis of the compound is made by reaction in solid-state and the size of grains after the final sintering is of several tens of microns. A new class of methods based on liquid-phase reaction to create a precursor containing all the cations of the final compound, which is subsequently precipitated and reduced to the final compound was also developed [2]. The compound obtained such way is amorphous, but after heat treatment at 600–800 °C it evolves to nanocrystalline material that can be transformed into transparent ceramic with grains of several microns (fine-grained ceramic) by sintering in vacuum at high temperature without need of isostatic compression. By using slip casting procedures this technique enables the mass production of very large ceramic bodies.

The fabrication process of the transparent polycrystalline laser materials implies temperatures 400–700 °C lower than for the melt-growth and is characterised by very high technological yield, high reproducibility and good control. Moreover, large bodies of size and shape close to that of the final optical component can be produced. These techniques have important potential for reduced production cost, very good use of the raw material and reduced energy consumption. The activity in the field is very intense and new progress is permanently reported [12–14].

The transparent polycrystalline laser materials show functional qualities that recommend them not only for substitution or extension of capabilities of known laser materials, but also for tailoring new laser materials or multifunctional materials due to the high compositional versatility; good control of composition, large doping concentrations, controlled profile of composition, doping or refraction index (homogeneous, gradient, mosaic, step change) over the whole volume of ceramic. Thus highly functional or monolithic composite ceramics consisting of parts with well-defined functions (active material, Q-switching material, material for suppression of the amplified spontaneous emission, materials that guide the pump radiation inside the laser material, materials that facilitate the heat dissipation) can be fabricated. The optical transmission and thermal conductivity of ceramics are similar to the single crystals, while the mechanical properties are considerably improved.

The high-resolution spectroscopy [9,15,16] revealed characteristics of the host ceramic and of the structural centers formed by the doping ions that are important for understanding and control of their laser properties:

- the variety, nature, and structure of the doping centers are similar to the corresponding single crystals;
- in the ceramics with micron or tens of micron grains the relative amount of defective structural centers (defective anionic coordination or symmetry, agglomerates or enhanced concentrations of doping ions) at or close to the grain surfaces is low compared with the total concentration of the doping ions and in many cases it can be neglected;
- in materials where the doping ion substitutes a host cation of similar valence the distribution of the "volume" doping ions at the available lattice sites is random;
- the quantum states of the doping ions (energy levels, transition probabilities) and their spectroscopic properties (positions and intensities of lines, radiative lifetimes) are similar to the single crystals;
- electron–phonon interaction similar to single crystals;
- ion–ion interactions and energy transfer processes similar to the single crystals;
- the melt-grown YAG crystals contain an excess of Y^{3+} ions that enter in the octahedral Al^{3+} sites a of the garnet. When placed in the vicinity of the doping ions, the $Y^{3+}(a)$ ions perturb the crystal field [17] inducing spectral satellites P_i whose intensity is proportional to the concentration of the $Y^{3+}(a)$ centers. In case of the Nd:YAG ceramics the intensities of the satellites P_i are much smaller than in the melt-grown crystals, indicating that their composition is much closer to the ideal garnet formula. The existence of these perturbed centers in crystals could let out from the laser process part of the doping ions; moreover, some of these satellites are lower in energy than the unperturbed centers and could act as traps for the excitation and reduce the laser efficiency. This could contribute to better laser performances of the ceramics than for crystals.

3. Lasers with ceramic active materials

The first demonstration of 1.064 nm laser emission with 1 at.% Nd:YAG ceramics [1] was soon followed by investigation of laser emission in more concentrated systems (4.6 at% Nd [18] and 6.9 at.% Nd [6] and recently 8 at.% [19]) under Ti:Sapphire laser pumping. The development of large fine-grained ceramic laser rods enabled the demonstration of 1.5 kW range CW laser emission under lamp pumping [20], with performances similar to the single crystals; subsequent improvement of the ceramics enabled superior performances. Diode laser pumping at 809 nm in the energy level $^4F_{5/2}$ of the conventional or composite ceramic Nd:YAG lasers demonstrated remarkable performances, such as 511 W from a composite1 at.% rod with transverse pumping [21], 144 W for end-pumped core-doped rod [22], 236 W quasi-CW emission with side-pumping [23], quasi-CW pumped, acousto-optically Q-switched emission with 42 W average output power [24] and 67 kW burst mode emission in a face pumped Nd:YAG ceramic heat capacity laser [4]. The Nd:YAG ceramic materials proved useful in non-linear devices as demonstrated by the 532 nm 104 W average power from an intracavity frequency-doubled Q-switched composite ceramic laser [25]. Lasers based on Nd or Yb emission in other ceramic materials, such as garnets or sequioxides have also been reported.

4. Further scaling of Nd-doped ceramic lasers

4.1. General consideration

For almost all the lasers with Nd-doped ceramic materials pumped by lamps or diode lasers in the 800 nm range the scaling to higher power or energy was hampered by severe thermal effects at high pumping. Further scaling imposes a correlated approach

that would account for the choice of material parameters, pumping conditions and laser design. The bases of this approach reside from the analysis of the effect of these factors on the partial efficiencies that determine the laser parameters and generation of heat. For more clarity this approach will be illustrated here for the case of the continuous-wave four-level lasers. The CW laser emission is characterised by two parameters, the emission threshold and the slope efficiency. Expressed vs. the absorbed pump power, these parameters are

$$P_{\rm th}^{(a)} = \frac{1}{2}\frac{Ah\nu_l}{\eta_p\eta_v\eta_{se}\tau_{rad}\eta_{qe}f_l\sigma_e\eta_{qd}^{(l)}}(T+L) \tag{1}$$

and respectively

$$\eta_{sl}^{(a)} = \eta_p\eta_v\eta_{se}\eta_{qd}^{(l)}\frac{T}{T+L} \tag{2}$$

When expressed in incident pump power these parameters become $P_{\rm th}^{(i)} = P_{\rm th}^{(a)}/\eta_a$ and $\eta_{sl}^{(i)} = \eta_{sl}^{(a)}\eta_a$, where $\eta_a = 1-\exp(-\alpha l)$, α being the absorption coefficient at the pump wavelength and l the effective path of the pump radiation inside the laser material. An optical–optical efficiency can also be defined

$$\eta_{o-o}^{(a)} = \frac{P_{out}}{P^{(a)}} = \eta_{sl}^{(a)}\left(1-\frac{P_{\rm th}^{(a)}}{P^{(a)}}\right) \tag{3}$$

In these equations η_p is the pump level efficiency that expresses the fraction of the laser ions excited by pump into the pump energy level that de-excite to the emitting level, η_v is the superposition efficiency of the laser mode volume and the pumped volume, η_{se} is the stimulated emission efficiency (the fraction of the excited ions in the emitting level that de-excite by stimulated emission), η_{qe} is the emission quantum efficiency (the fraction of excited ions that de-excite by radiative processes (luminescence) in absence of laser emission), τ_{rad} is the spontaneous radiative lifetime of the emitting level, f_l is the fractional thermal coefficient for the emitting level, σ_e is the emission cross-section, $\eta_{qd}^{(l)} = \lambda_p/\lambda_l$ is the quantum defect (Stokes) ratio between the emission quantum and pump quantum and A is the laser beam cross-section.

Owing to the particularities of the laser emission process (existence of threshold, superposition efficiency that can be less than the unity) only part of the ions excited to the emitting level, defined by the laser efficiency $\eta_l = \eta_v\eta_{se}(1-f_{\rm th})$ participate to the laser emission; here $f_{\rm th} = P_{\rm th}/P$ represents the fraction of the excited ions at the laser threshold. The fraction of absorbed power that is converted to the laser emission is given by

$$\eta^{(l)} = \eta_p\eta_l\eta_{qd}^{(l)} = (1-f_{\rm th})\eta_p\eta_v\eta_{se}\eta_{qd}^{(l)} \tag{4}$$

Part of the ions that do not participate to lasing de-excite by luminescence and the rest by non-radiative processes (energy transfer, electron–phonon interaction) that can result in heat generation. The part of absorbed power that is converted to luminescence emission is

$$\eta^{(f)} = (1-\eta_l)\eta_p\eta_{qe}\eta_{qd}^{(f)} \tag{5}$$

where $\eta_{qd}^{(f)} = \lambda_p/\bar{\lambda}$ is the quantum defect ratio for the luminescence emission with average wavelength $\bar{\lambda}$. The part of absorbed power transformed into heat (the fractional thermal load coefficient) is then

$$\eta_h = 1-\eta_p\eta_l\eta_{qd}^{(l)} - (1-\eta_l)\eta_p\eta_{qe}\eta_{qd}^{(f)} \tag{6}$$

The heat load parameter includes the specific contribution to heating from the ions that participate to lasing and from those that do not participate. Two limiting cases of Eq. (6) refer to the heat generation in absence of laser emission ($\eta_l = 0$) when $\eta_h^{(f)} = 1-\eta_p\eta_{qe}\eta_{qd}^{(f)}$ and at very high laser efficiency ($\eta_l = 1$) when $\eta_h^{(l)} = 1-\eta_p\eta_{qd}^{(l)}$: it is obvious that for materials and pump and laser wavelengths for which $\eta_{qd}^{(l)} \succ \eta_{qd}^{(f)}\eta_{qe}$ the ions that participate to lasing generate less heat than those that do not participate.

The laser materials and the pumping conditions could be selected to grant high partial efficiencies suitable for efficient laser emission and low heating. For a given laser material and laser emission scheme ($\nu_p, \sigma_e, \nu_l, \tau_{rad}, f_l$):

- wavelength of pump close to that of the laser determines large quantum defect ratios $\eta_{qd}^{(l)}$ and $\eta_{qd}^{(f)}$ whereas large pumping intensities ($P/P_{\rm th}$) increase the laser efficiency η_l;
- the selection of the material (doping concentration, size) implies high absorption efficiency η_a and high emission quantum efficiency η_{qe} as well as low residual losses L;
- the laser design determines A, η_v, and T and could also influence η_a by recirculation of pump in the material.

A pump wavelength, as close as possible to that of the laser would determine higher laser parameters and less heat generation. Since the laser transition for the four-level lasers implies a laser terminal level above the ground level, i.e. the existence of a lower (down)-quantum defect, this condition can be realized by reducing the upper quantum defect between the pump energy level and the emitting level or by eliminating it with direct pumping into the emitting level. Traditionally the diode pumping of Nd lasers is made at ~800 nm (809 nm for Nd:YAG) in the strongly absorbing energy level $^4F_{5/2}$, placed 800–900 cm^{-1} above the emitting level $^4F_{3/2}$ and this energy difference is transformed into heat. In many important laser materials such as the garnets the cross-section of the absorption into the emitting level $^4F_{3/2}$ is quite low and special care to increase the absorption efficiency by using more concentrated materials and/or larger rods as well as by recirculation of the pump radiation inside the laser material (multi-pass pumping, zigzag configurations, guiding) must be taken. With the advent of the transparent ceramics very high doping concentrations (up to 9 at.%) of Nd in YAG become possible. In case of YAG the absorption spectrum $^4I_{9/2} \rightarrow {}^4F_{3/2}$ contains two absorption bands suitable for pumping, $Z_1 \rightarrow R_1$ band at 869 nm (linewith smaller than 1 nm for 1 at.% Nd) and a double-peaked band (total linewidth 2.5 nm) centered at 885 nm that collects the absorption lines $Z_2 \rightarrow R_1$ and $Z_3 \rightarrow R_2$. At the room temperature the fractional thermal population coefficients for the Stark levels from which the absorption takes part (f_1 for the 869 nm and 809 nm lines and $f_2 + f_3$ for the 885 nm band) are almost equal; however, with 100 °C increase of temperature the first drops by ~15%, while the second increases by ~5% indicating a more stable pump absorption efficiency. The 300 K peak absorption coefficient for the 885 nm absorption band (1.7 cm^{-1} for 1 at.% Nd) is much smaller than for the sharp 809 nm absorption line (11.4 cm^{-1}); however in case of quite narrow (~2 nm) diode laser pumping the ratio of the effective absorption coefficients (~5 cm^{-1} and respectively ~1.3 cm^{-1}) is smaller.

The CW 1064 nm laser emission under direct 885 nm pumping in the emitting level of Nd^{3+} in YAG ceramics (with up to 6.8 at.% Nd) was demonstrated with Ti:sapphire laser pumping [6] and subsequently with diode laser pumping [26]. The laser parameters (slope efficiency and threshold) are considerably improved compared with the traditional 809 nm pumping. The improvement was generally larger than 9.5% predicted by the quantum defect ratio, due to the additional contribution of the reduced heat generation and of the increased beam quality. The comparative investigation of the laser emission in Nd:YAG crystals and ceramics up to ~3.8 at.% Nd shows that the performances of these two types of materials are similar.[3,27]. Recently CW emission in the 250–275 W range with longitudinal 885 nm diode laser pumping of

long diluted Nd:YAG composite ceramic rods with one or two-doped regions was reported [28,29].

The high Nd concentrations can reduce the emission quantum efficiency due to the energy transfer inside of the system of Nd ions. At low excitation the self-quenching is dominated by cross-relaxation energy transfer between an excited Nd^{3+} ion and another Nd^{3+} ion in its ground state, $(^4F_{3/2}, {}^4I_{9/2}) \rightarrow (^4I_{15/2}, {}^4I_{15/2})$. At high pump intensities in absence of laser emission, additional de-excitation processes due to upconversion become gradually important. The C_{Nd} dependence of emission quantum efficiency can be calculated by using the characteristic parameters of the energy transfer determined from the concentration effects in the emission decay of Nd. It was thus shown that in case of Nd-doped YAG [9] and GSGG [10] the energy transfer processes in crystals and ceramics are identical: at low Nd concentrations this is dominated by direct (static) donor-acceptor transfer caused by superexchange and electric dipole–dipole interactions between the Nd ions, whereas with increasing Nd concentration migration-assisted transfer becomes important. A similar picture was observed in case of Nd:Y_2O_3 ceramic [30]. The C_{Nd} dependence of emission quantum efficiency at low excitation, calculated with the energy transfer parameters inferred from the emission decay for Nd:YAG and Nd:GSGG is shown in Fig. 1. These values describe very well the experimental data measured up to 3.4% Nd in YAG by various techniques such as interferometry [31], heating [32] and thermally induced depolarisation [33], by assuming $\eta_p = 1$.

The direct 885 nm pumping increases the quantum defect ratios $\eta_{qd}^{(l)}$ and $\eta_{qd}^{(f)}$ by ~9.5% compared with the 809 nm traditional pumping; however, the effect on heat generation is much larger. Thus, for efficient 1064 nm laser emission ($\eta_l = 1$) the heat loading parameter $\eta_h^{(l)}$ decreases from ~0.24 to 0.168 i.e. by about 30% regardless the Nd concentration, whereas in case of $\eta_h^{(f)}$ the effect depends on C_{Nd} via η_{qe}: for 1 at.% Nd:YAG the decrease is from 0.376 to 0.32 i.e. only 15.5%. For the general case, the heat loading parameter takes intermediate values: Fig. 2 shows the dependence of η_h on the intensity of pumping for various Nd concentrations in YAG assuming superposition efficiency $\eta_v = 1$. The value 1 on the absorbed power scale corresponds to 1 at.% Nd and the threshold values for each Nd concentration are calculated using Eq. (1) It is thus evident that the limiting $\eta_l = 1$ case and thus the $\eta_h^{(l)}$ value holds only to very high pumping intensities; however, the heat loading parameter for a given pump intensity is always smaller in case of the 885 nm than for 809 nm pumping. Lower than the unity η_v determines enhancement of η_h.

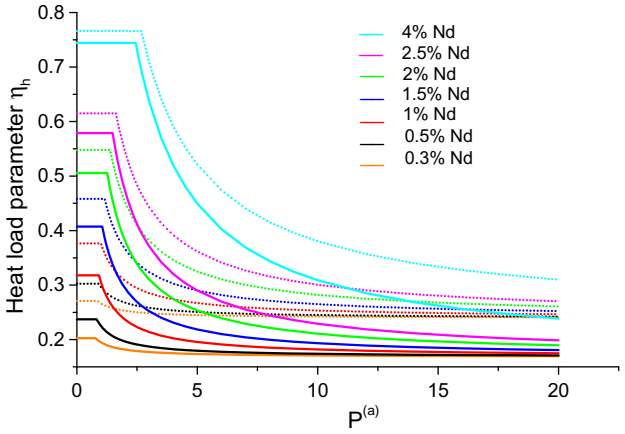

Fig. 2. Heat load parameter for Nd:YAG under 809 nm (dotted line) and 885 nm (full line) pumping.

4.2. The effect of the pump wavelength on the laser parameters

The consideration of the effect of material and pumping characteristics on the laser parameters can be facilitated by using appropriate figures-of-merit (F-o-M): most significant is F-o-M for the optical-optical efficiency $\Phi_{o-o}^{(a)} = \eta_{qd}^{(l)}(1 - P_{th}/P)$ and $\Phi_{o-o}^{(i)} = \eta_a \Phi_{o-o}^{(a)}$. In case of CW laser emission, the low inversion at threshold grants the validity of the emission quantum efficiencies given in Fig. 1 for estimation of these figures-of-merit. The F-o-M $\Phi_{o-o}^{(a)}$ function of pump intensity for Nd:YAG is given in Fig. 3 and is always larger for 885 nm than for 809 nm pumping, the largest values being obtained for the less concentrated materials

For practical cases $\Phi_{o-o}^{(i)}$ is of relevance and this depends also on the absorption efficiency, i.e. on the effective path of pump radiation inside the laser material. From Fig. 4 is evident that for short absorption path l (such as 0.5 cm) pumping at 809 nm proves more efficient than 885 nm; however, with increasing of l (such as 2.5 cm) the 885 nm diode pumping becomes more efficient. Further increase of l enables reduction of Nd concentration, resulting in lowering of emission threshold and to the increase of the optical-optical efficiency. As discussed above, scaling in power implies simultaneous increase of the laser parameters and the reduction of heat generation. The effect of the various material, pumping system and laser design parameters can be accounted for with a generalised figure-of-merit $\Phi_{gen} = \Phi_{o-o}/\eta_h$. Fig. 5 shows the

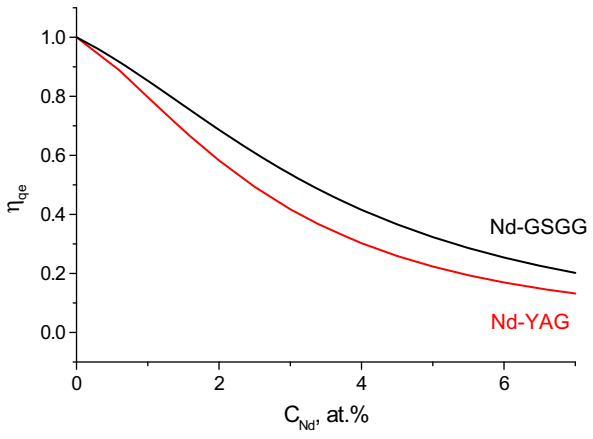

Fig. 1. Calculated emission quantum efficiency for Nd:YAG and Nd:GSGG.

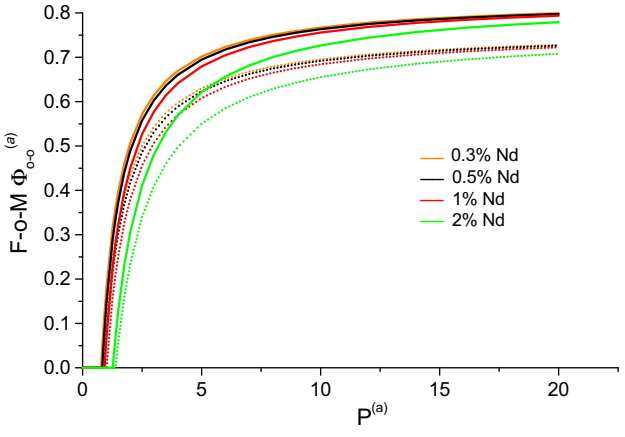

Fig. 3. The optical-optical F-o-M in absorbed power for Nd:YAG with 809 (dotted line) and 885 nm (full line) pumping.

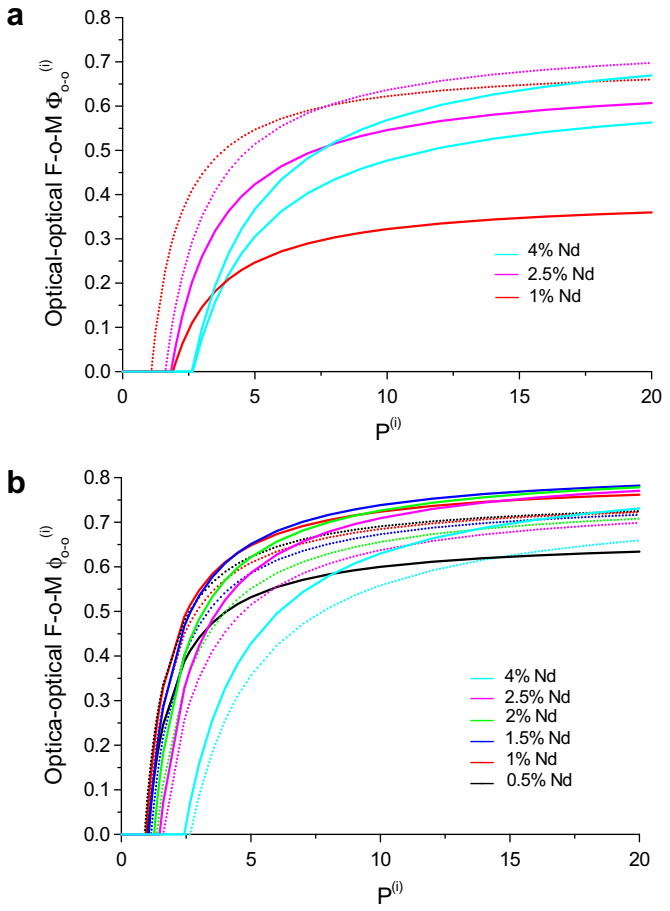

Fig. 4. The optical-optical figure of merit in incident power for effective absorption paths 0.5 cm (a) and 2.5 cm (b) under 809 nm (dotted line) and 885 nm (full line) diode pumping.

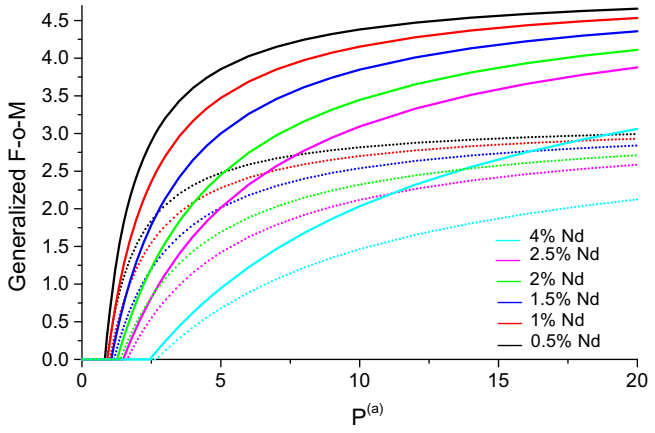

Fig. 5. The generalised F-o-M in absorbed power for Nd:YAG.

generalised F-o-M $\Phi_{gen}^{(a)}$ for Nd:YAG, whereas Fig. 6 gives $\Phi_{gen}^{(i)}$ for absorption paths of 0.5 and 2.5 cm.

Fig. 5 shows that the direct diode laser pumping at 885 nm of Nd:YAG enables, in principle the best use for laser emission of the absorbed pump radiation, the ratio of the power found in the laser emission to that transformed into heat being about 60–70% larger than for the traditional 809 nm pumping and for both pump

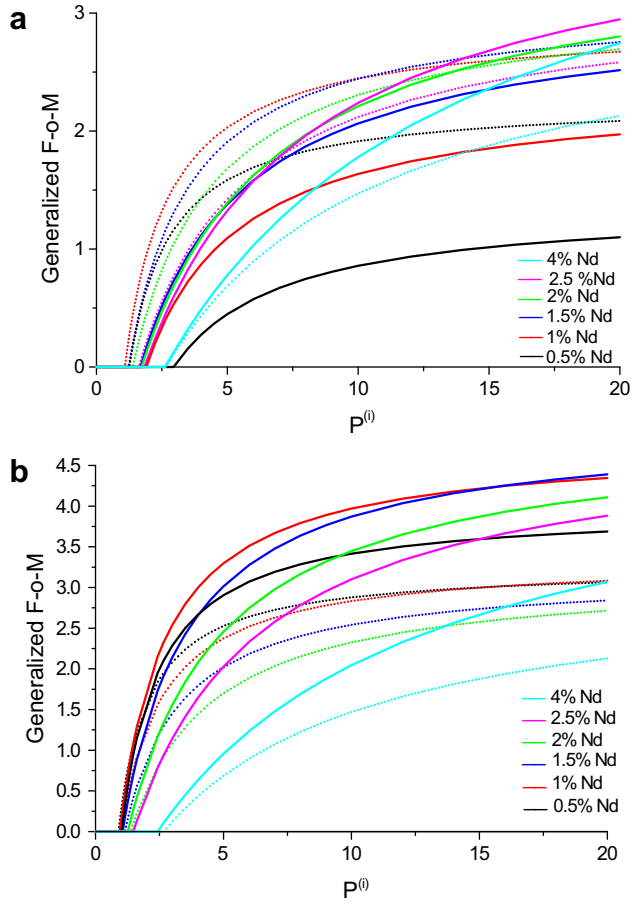

Fig. 6. The generalised F-o-M for Nd:YAG for effective absorption paths 0.5 cm (a) and 2.5 cm (b).

wavelengths the largest ratio is obtained for the lower Nd concentrations. However, the extent to which such potential can be used in practice depends on the absorption efficiency. As shown in Fig. 6, in case of short absorption paths, for which the absorption efficiency for the 885 nm pump is weaker, the generalised F-o-M is larger for the 809 nm pumping in the region of weak and moderate pump intensity, but becomes favourable to 885 nm pumping in concentrated materials at high pump intensity. For the 2.5 cm path the direct 885 nm pumping appears more favorable, the best performance being obtained for ~1.6% Nd. With increasing of the path l, i.e. of the pump absorption efficiency, the situation approaches more and more the picture obtained in absorbed power and the best performances are gradually obtained for lower Nd concentrations. Thus, for an absorption path of 10–12 cm, the best performance would be obtained with the 885 nm diode pumping of 0.3% Nd:YAG.

4.3. The concept of power scaling

The concept of power scaling is illustrated in Fig. 7 that represents the power found in the ideal laser emission ($\eta_v = 1$, material with very low residual losses, $L \approx 0$) and the power transformed into heat for a Nd:YAG rod with $l = 2.5$ cm. If the scaling of the laser is limited to a thermal power of 3.15, this can be generated in case of 809 nm by pumping at an incident power of 12 (the units are expressed relative to the threshold for a 1 cm long 1% Nd rod) that enable emission of 8.25 units, whereas in case of 885 nm pumping this amount of heat is generated for a much larger pump power (18), that enable emission of 13.8 units. This reflects a potential

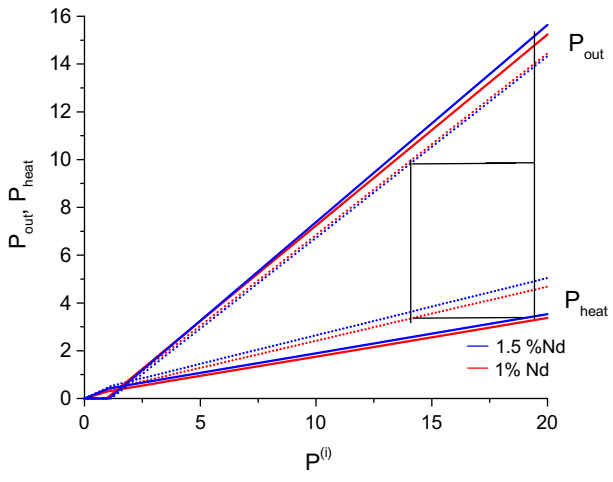

Fig. 7. Illustration of the concept of power scaling for the Nd:YAG lasers ($l = 2.5$ cm).

of laser emission by ~65% larger for 885 nm pumping for similar heat generation.

5. Discussion and conclusion

The ceramic laser materials enable a considerable extension of the performances and varieties of solid-state lasers. This study illustrates on the case of Nd:YAG that a correlated approach of the laser material, conditions of pumping and details of the laser design enable a considerable scaling in power of the lasers. The conclusion of this study can be used directly in case of other Nd lasers in relaxed regime, such as long pulse emission. This indicates that the high power lasers, such as the large-aperture heat capacity lasers or the zig-zag CW lasers can be scaled in power by more than 50–60% by simply replacing the pumping system from 809 nm to 885 nm, without the need of additional rods. The 885 nm pumping offers the additional advantage of more stable emission over larger temperature range and of more uniform pump distribution inside the laser material. This concept can be extended simply to lasers with storage of excitation such as in the Q-switched emission, or to amplifiers, by a proper account of the effects of upconversion on the dynamics of excitation below the emission threshold.

References

[1] A. Ikesue, K. Kamata, K. Yoshida, J. Am. Ceram. Soc. 78 (1995) 225.
[2] J. Lu, M. Prabhu, J. Song, C. Li, J. Xu, K. Ueda, A.A. Kaminskii, H. Yagi, T. Yanagitani, Appl. Phys. B 71 (2000) 469.
[3] V. Lupei, N. Pavel, T. Taira, IEEE J. Quantum Electron. 38 (2002) 240.
[4] R.M. Yamamoto, C.D. Booley, K.P. Cutter, S.N. Fochs, K.N. LaFortune, J.M. Parker, P.H. Paks, M.D. Rotter, A.M. Rubenchik, T.F. Soules, Proc. SPIE 6552 (2007) 655205.
[5] R. Lavi, S. Jackel, Appl. Opt. 39 (2000) 3093.
[6] V. Lupei, A. Lupei, N. Pavel, I. Shoji, T. Taira, A. Ikesue, Appl. Phys. Lett. 79 (2001) 590.
[7] V. Lupei, N. Pavel, T. Taira, Appl. Phys. Lett. 81 (2002) 2677.
[8] V. Lupei, Opt. Mater. 24 (2003) 353.
[9] V. Lupei, A. Lupei, S. Georgescu, T. Taira, Y. Sato, A. Ikesue, Phys. Rev. B 64 (2001) 092102.
[10] V. Lupei, A. Lupei, C. Gheorghe, A. Ikesue, J. Luminesc. 128 (2008) 885.
[11] A. Ikesue, K. Kamata, K. Yoshida, J. Am. Ceram. Soc. 79 (1996) 359.
[12] A. Ikesue, Y.L. Aung, T. Taira, T. Kamimura, K. Yoshida, G.L. Messing, Ann. Rev. Mater. Sci. 36 (2006) 397.
[13] H. Yagi, T. Yanagitani, K. Takaichi, K.I. Ueda, A.A. Kaminskii, Opt. Mater. 29 (2007) 1258.
[14] A. Ikesue, Y.L. Aung, T. Yoda, S. Nakayama, T. Kamimura, Opt. Mater. 29 (2007) 1289.
[15] V. Lupei, A. Lupei, S. Georgescu, B. Diaconescu, T. Taira, Y. Sato, S. Kurimura, A. Ikesue, J. Opt. Soc. Am. B 19 (2002) 360.
[16] V. Lupei, A. Lupei, A. Ikesue, J. Alloys Compd. 380 (2004) 61.
[17] A. Lupei, V. Lupei, E. Osiac, J. Phys.:Condens. Mat. 10 (1998) 9701.
[18] I. Shoji, S. Kurimura, Y. Sato, T. Taira, A. Ikesue, K. Yoshida, Appl. Phys. Lett. 77 (2000) 939.
[19] L.D. Merkle, M. Dubinskii, K.L. Schlepler, S.M. Hedge, Opt. Express 14 (2006) 3893.
[20] J. Lu, K. Ueda, H. Yagi, T. Yanagitani, Y. Akiyama, A.A. Kaminskii, J. Alloys. Compd. 341 (2002) 220.
[21] H.F. Li, D.G. Xu, Y. Yang, Chinese Phys. Lett. 22 (2005) 2575.
[22] D. Kracht, D. Freiburg, R. Wilhelm, M. Frede, C. Fallnick, Opt. Express 14 (2006) 2690.
[23] Y. Qi, X. Zhu, Q. Lou, J. Ji, J. Dong, Y. Wei, Opt. Express 13 (2005) 8725.
[24] T. Omatsu, K. Nawata, D. Sauder, A. Minassian, M.J. Damzen, Opt. Express 14 (2006) 9198.
[25] D. Xu, Y. Wang, H. Li, J. Yao, Y.H. Tsang, Opt. Express 15 (2007) 3991.
[26] V. Lupei, N. Pavel, T. Taira, Appl. Phys. Lett. 80 (2002) 4309.
[27] V. Lupei, A. Lupei, N. Pavel, T. Taira, A. Ikesue, Appl. Phys. B73 (2001) 757.
[28] M. Frede, R. Wilhelm, D. Kracht, Opt. Lett. 31 (2006) 3618.
[29] M. Frede, D. Freiburg, R. Wilhelm, D. Kracht, Proc. SPIE 6451 (2007) 64510G.
[30] A. Lupei, V. Lupei, T. Taira, Y. Sato, A. Ikesue, C. Gheorghe, J. Luminesc. 102–103 (2003) 72.
[31] K.K. Deb, R.G. Buser, J. Paul, Appl. Opt. 20 (1981) 1203.
[32] T.Y. Fan, IEEE J. Quantum Electron. 29 (1993) 1457.
[33] I. Shoji, Y. Sato, S. Kurimura, V. Lupei, T. Taira, A. Ikesue, K. Yoshida, Opt. Lett. 27 (2002) 234.